Condition Monitoring of Power Semiconductors by Means of the Controller Output Voltage Harmonics

Firat Yüce[1], Marc Hiller[1]

[1] Karlsruhe Institute of Technology (KIT), Institute of Electrical Engineering (ETI), Germany

Corresponding author: Firat Yüce, firat.yuece@kit.edu

Abstract

In this publication, a novel approach for condition monitoring of power semiconductors is presented. The approach requires no additional sensors and only uses the data that is already available in a power electronic system. The method is based on the analysis of the output control variables of the current controller. Therefore, firstly, the effects of the sensitive parameters that provide information about aging of the power semiconductors on the controller outputs are analysed. This is done by power converter models that allow the variation of sensitive power semiconductor parameters. Based on these results, models are set up, which allow the calculation of sensitive parameters during converter operation - and thus the condition of the power semiconductors. Measurements are performed on the test bench in which the controller outputs are recorded. The chip temperatures of the power semiconductors are measured with a thermal imaging camera in order to evaluate the temperature related effects. Finally, an algorithm is proposed that is able to detect an anomaly of the power semiconductors. The algorithm can even conclude the aging mechanism by detection of a change in the sensitive parameters. Furthermore, detailed data analysis can determine which chip exactly is damaged.

1 Introduction

Power electronics is a key technology for sustainable energy production and environmentally-friendly mobility. The requirements for power electronics such as power and energy density are steadily increasing. Due to an increased use of power electronics in drive technologies the reliability of these systems and its components is becoming increasingly important.

One possibility to increase the reliability of power electronic systems is to use condition monitoring. Conditiong monitoring has the goal of identifying the condition of a system during operation and thus providing information for necessary repair and maintenance work. This information enables the selection of optimal maintenance intervals in order to reduce the downtimes of a plant. For example, the availability of wind turbines can be increased if it is known when the converter requires maintenance. As a result, maintenance costs can be reduced and downtimes can be better planned, especially for offshore wind turbines, which are difficult to access.

2 State of the art

So far, there are two approaches of condition monitoring of power converters.

One approach deals with the monitoring of sensitive parameters. Sensitive parameters provide information about the condition of the converter. This approach is able to detect all aging mechanisms affecting the sensitive parameter. A sensitive parameter can either be measured directly or indirectly. Direct measurements make use of a measurement circuit, while indirect measurements use model estimations. Usually, both methods require additional measurement equipment.

There are several research publications that propose a methodology for estimating sensitive parameters for the purpose of condition monitoring. In [1], a measurement circuit was developed that measures the collector-emitter voltage of the IGBT in the on state and thus can detect the aging mechanism *bond wire lift-off*. In [2], a method is presented to detect the aging mechanisms *solder fatigue* and *bond wire lift-off*. This is done by online monitoring of the two sensitive parameters:

thermal resistance between junction and heatsink R_{th} and differential resistance of the collector-emitter path r_{CE}, which are estimated by an indirect method using a measurement circuit. In [3], these two aging mechanisms are detected by estimating the chip temperature. Since the chip temperature cannot be measured directly, it is calculated using an analog measurement circuit that evaluates the turn-off time of the IGBT. Additionally to the forementioned, the *contamination of the cooling system* is investigated in [4]. This shows that other components beyond the power semiconductors, such as the cooling system, can also be monitored by selecting suitable sensitive parameters. For this purpose, low-frequency power losses are applied to the IGBT for a short time during operation. Then, the temperature cycles are determined and the maximum and minimum values of the chip temperature are evaluated. These temperatures are calculated using a thermal model. An increase in the maximum temperature indicates the aging mechanism *solder fatigue* and an increase in the minimum temperature indicates the aging mechanism *contamination of the cooling system* [4].

Another approach is model-based aging prediction, which has the aim of physically modeling a specific aging mechanism that leads to converter failure. This approach requires detailed knowledge of the aging process and can only detect the modeled aging mechanism. For example, the aging mechanism loss of blocking capability due to increased leakage currents because of *humidity* can be modeled using thermo-mechanical and electrochemical models [5]. These models are used during converter operation in order to estimate the current condition and the remaining lifetime.

A major disadvantage of the existing methods of condition monitoring is the need for additional sensors and measuring equipment, which entails additional costs and sources of failure. The proposed approach overcomes this disadvantage and operates without additional hardware. This results not only in a significant cost advantage, but also in a higher reliability of the power converter system due to the elimination of additional potential sources of failure. Therefore, the already available operating data is analyzed for certain patterns and characteristics. Additional effort only results from the increased need for computing power in the signal processing of the converter system.

3 Modelling

In this paper, a three-phase two-level converter is investigated. It is a widely used circuit, which is applied, for instance, in electric vehicles, industrial machines, wind and solar power systems. Figure 1 shows the circuit topology with a resistive-inductive load connected to it. The converter should first be investigated independently of the interactions with a complex load such as an electrical machine or other external components.

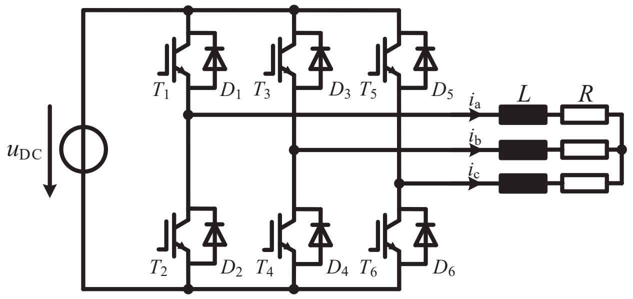

Fig. 1: Three-phase two-level bridge

3.1 Ideal Converter Model

The aim is to describe the circuit topology with the help of differential equations and then to transfer these into the state space representation, which is suitable for the system description of a transfer function. The state space representation is described by the first order state differential equation (1) and by the output equation (2).

$$\dot{\vec{x}} = A \cdot \vec{x} + B \cdot \vec{u} \tag{1}$$

$$\vec{y} = C \cdot \vec{x} \tag{2}$$

Here $\vec{x}$ denotes the state variable, $\vec{y}$ the output variable and $\vec{u}$ the input variable. The coefficients A, B and C are matrices. The state variable $\vec{x}$ contains the load-side currents (3). The output variable $\vec{y}$ is identical with the state vector $\vec{x}$ - consequently the matrix C represents the unit matrix. The dc link voltage u_{DC} is the input variable of the system $\vec{u}$.

$$\vec{x} = \begin{pmatrix} i_{\mathrm{a}} \\ i_{\mathrm{b}} \\ i_{\mathrm{c}} \end{pmatrix} \qquad \vec{y} = \begin{pmatrix} i_{\mathrm{a}} \\ i_{\mathrm{b}} \\ i_{\mathrm{c}} \end{pmatrix} \qquad \vec{u} = \begin{pmatrix} u_{\mathrm{DC}} \end{pmatrix} \tag{3}$$

The two matrices A and B are to be identified. Firstly, the entire state space equation (1) is multiplied by the matrix E, resulting in equation (4). This mathematical operation leads to a coefficient in front of each variable of the state differential equation, which simplifies the comparison of coefficients with the differential equations.

$$E \cdot \dot{\vec{x}} = F \cdot \vec{x} + G \cdot \vec{u} \tag{4}$$

The two matrices that have to be identified are given in (5).

$$A = E^{-1} \cdot F \qquad\qquad B = E^{-1} \cdot G \tag{5}$$

As an ideal model is described, all power semiconductor components are considered to be ideal. The transistors are assumed to be ideal switches S, which take the value 1 when the switch is closed and the value 0 when the switch is open. Three differential equations are set up - two voltage equations and one current equation. The equations are not further elaborated here. Then, these differential equations are transformed into the state form (4) by a coefficient comparison. This results in the matrices shown in (6) - (9).

$$E = \begin{pmatrix} -L_\mathrm{a} & L_\mathrm{b} & 0 \\ 0 & -L_\mathrm{b} & L_\mathrm{c} \\ 1 & 1 & 1 \end{pmatrix} \tag{6}$$

$$C = \begin{pmatrix} 1 & 0 & 0 \\ 0 & 1 & 0 \\ 0 & 0 & 1 \end{pmatrix} \tag{7}$$

$$F = \begin{pmatrix} R_\mathrm{a} & -R_\mathrm{b} & 0 \\ 0 & R_\mathrm{b} & -R_\mathrm{c} \\ 0 & 0 & 0 \end{pmatrix} \tag{8}$$

$$G = \begin{pmatrix} -\frac{(S_1 - S_2) - (S_3 - S_4)}{2} \\ -\frac{(S_3 - S_4) - (S_5 - S_6)}{2} \\ 0 \end{pmatrix} \tag{9}$$

3.2 Converter Model with Sensitive Parameters

In the previous chapter 3.1, the power converter is modeled as a state space model with the equation (4) and the corresponding matrices (6) - (9). The aim of this chapter 3.2 is now to extend this model by some sensitive parameters. These parameters are represented by physical equivalent circuit elements in the power converter model.
The conduction characteristics of the power semiconductor devices are simulated by the two parameters r_on and U_f, where r_on represents the differential resistance and U_f the threshold voltage of the collector-emitter path. This is an initial selection of sensitive parameters. The model can be extended by further parameters. The i_CE - u_CE conduction characteristic of a power semiconductor device with the two parameters r_on and U_f can be described by equation (10).

$$u_\mathrm{CE} = U_\mathrm{f} + r_\mathrm{CE} \cdot i_\mathrm{CE} \tag{10}$$

The resulting equivalent circuit with the modeled conduction characteristics of the power semiconductor devices can be seen in Fig. 2.

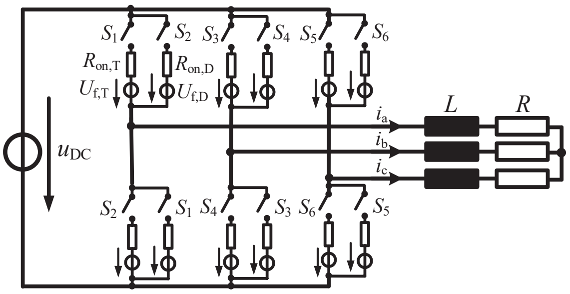

Fig. 2: Three-phase two-level bridge with sensitive parameters

In equation (11) the new form of the state space equations is shown.

$$E \cdot \dot{\vec{x}} = F \cdot \vec{x} + G \cdot \vec{u} + Z \tag{11}$$

Here, the new term Z is added. According to the procedure of chapter 3.1, the differential equations are set up for the model with sensitive parameters. Subsequently, these equations are transformed into the new form of the state space representation (11). The matrices E, F, G and Z result in (12) to (15).

$$E = \begin{pmatrix} -L_\mathrm{a} & L_\mathrm{b} & 0 \\ 0 & -L_\mathrm{b} & L_\mathrm{c} \\ 1 & 1 & 1 \end{pmatrix} \tag{12}$$

$$G = \begin{pmatrix} -\frac{(S_1-S_2)-(S_3-S_4)}{2} \\ -\frac{(S_3-S_4)-(S_5-S_6)}{2} \\ 0 \end{pmatrix} \tag{13}$$

$$F = \begin{pmatrix} R_\mathrm{a} + F_1 & -R_\mathrm{b1} - F_2 & 0 \\ 0 & R_\mathrm{b} + F_2 & -R_\mathrm{c} - F_3 \\ 0 & 0 & 0 \end{pmatrix} \tag{14}$$

$$Z = \begin{pmatrix} Z_1 - Z_2 \\ Z_2 - Z_3 \\ 0 \end{pmatrix} \tag{15}$$

Unlike the matrices (6) - (9) from equation (4), the matrices (12) - (15) have additional terms, which depend on the sign of the phase current. A case distinction must be made for different signs of the phase currents, since either the IGBT or the diode conducts depending on the current sign.

4 Test bench

The test bench consists of a simple structure (Fig. 3). The reduced external influences allow concentration on the development of methods for condition monitoring of the power semiconductor itself. Hence, a passive RL-load is used.

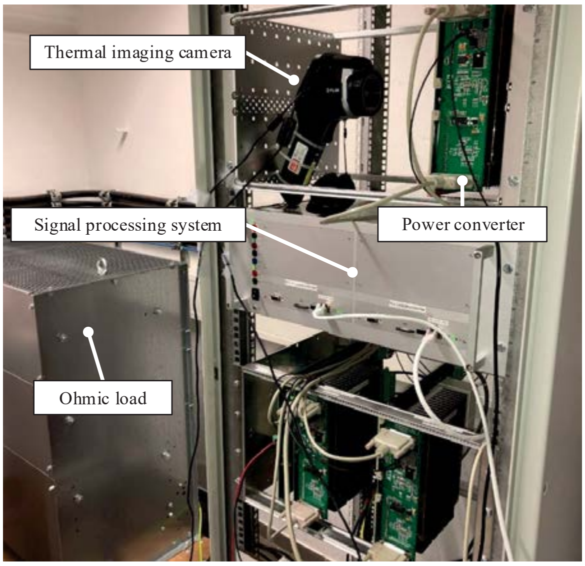

Fig. 3: Test bench

The converter is equipped with the IGBT module Infineon EconoPack2 FS75R12KT4 ($1200\,\mathrm{V}/75\,\mathrm{A}$) and has a nominal power of $30\,\mathrm{kW}$ at a switching frequency of $8\,\mathrm{kHz}$. The test bench provides a measuring system for the three-phase output currents and the DC link voltage. Furthermore, the module temperature is measured by an NTC resistor. The test bench enables the intentional implementation of fault cases. In order to gain access to the power semiconductor chips and to measure the chip temperature during converter operation, an opening window has been designed in the circuit board of the power converter (Fig. 4). Possible failure mechanisms that can be implemented include heating of individual chips with a hot air gun, cutting off individual bond wires (bond wire lift-off) and performing accelerated life tests. The chip temperature is measured using the FLIR E60 thermal imaging camera (Fig. 4).

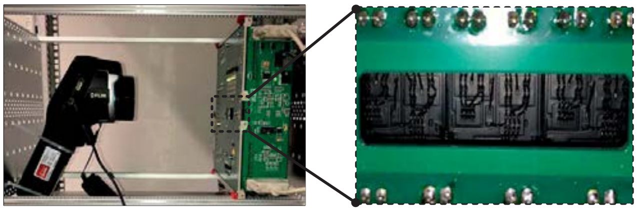

Fig. 4: Open viewing window in the circuit board

5 Failure detection algorithms

The approach to condition monitoring is shown in Fig. 5. The approach starts with the data acquisition. Here, the relevant data for fault detection is saved. In this work, all output control variables of the control system are collected. In the next step, a data preprocessing is applied in which an outlier elimination is performed. Statistical methods are used to detect those data points that show significant deviation from the other data points in order to eliminate them from the data set. Subsequently, the processed data is passed into the data analysis, which consists of a two-step procedure: anomaly detection and root cause detection. The anomaly detection model aims to detect an anomaly within the data set. This algorithm is trained with real data, also considering environmental and operating conditions such as the measured module temperature. Within this process, a classification algorithm is used, deciding whether an anomaly has occured or not. An anomaly does not necessarily have to be aging. For example, if there is an environmental condition unknown to the algorithm, this can also lead to an anomaly within the data set. In practical applications, an additional mechanism between the anomaly detection model and the root cause detection model is required to decide whether aging or some other change has occurred. If this decision process concludes that aging has occurred, then the data set is passed to the root cause detection model. The goal of the root cause detection model is to both, locate the cause of the aging and determine the severity of the aging. The root cause detection model is trained with simulation data. The simulation models developed in chapter 3.2 are used to simulate specific failure mechanisms. Based on these simulations, models are trained that are able to detect these failure mechanisms. In the following, the various points of the approach are discussed.

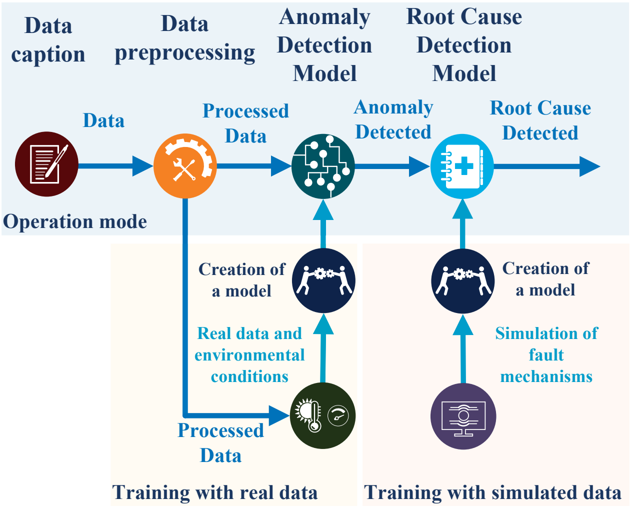

Fig. 5: Approach to condition monitoring and failure detection

5.1 Data caption

Instead of analyzing the sensor data, the controller output variables are considered. The information content in the data recorded by the sensors is much less, as these values are forced to the desired set point by the control system. The controller always reacts to changes of the system. This means that the controller also reacts to aging of the system components. This principle is used to detect aging mechanisms that have occurred during operation. In [6], the current control system is shown. The output voltages and can be divided into a d- and a q-component, which represent the d- and q-axis in the rotational reference system. In addition, the output variables of the control are divided into proportional and integral components, of which each can represent different types of failures due to their different characteristics. The signals are analysed in the frequency domain. For this purpose, a Fast Fourier Transformation (FFT) is performed for each electrical period to transform the voltages from the time domain to the frequency domain. The operating point is given in Tab. 1.

Parameter	Value
Current d-axis i_d	$10\,\mathrm{A}$
Current q-axis i_q	$0\,\mathrm{A}$
DC link voltage U_DC	$200\,\mathrm{V}$
Electrical frequency f_el	$50\,\mathrm{Hz}$
Sample frequency f_S	$16\,\mathrm{kHz}$
Ohmic resistors $R_\mathrm{a}, R_\mathrm{b}, R_\mathrm{c}$	$2,1\,\Omega$
Load inductors $L_\mathrm{a}, L_\mathrm{b}, L_\mathrm{c}$	$2\,\mathrm{mH}$

Tab. 1: Parameter set of operating point

The data set consists of almost 600 data points since this is the number of electrical periods that are captured. Figure 6 shows the 6^th and 12^th harmonic of the integral part of the controller output in q-axis for the investigated operating point. These data points are used to demonstrate the working principle of the different processes given in Fig. 5.

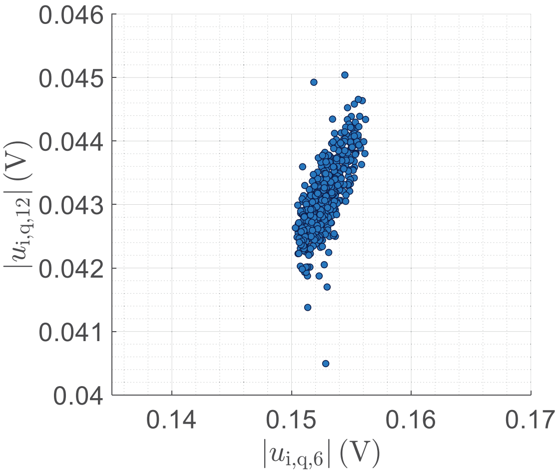

Fig. 6: 6^th and 12^th harmonics of the integral part

5.2 Data preprocessing

Since a measurement usually contains outliers, statistical methods are used to remove these unwanted data points. For this purpose, the algorithm „Fast Algorithm for the Minimum Covariance Determinant Estimator“ algorithm is used [7]. In Fig. 7, the mathematical model of the outlier detection, which has the shape of an ellipse, is shown.

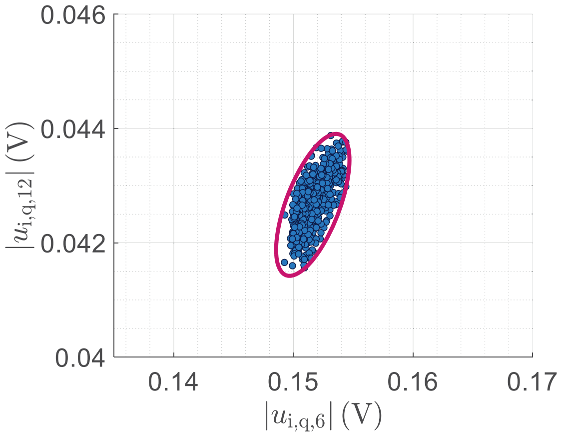

Fig. 7: Outlier detection

The operating principle of the algorithm is to find a robust mean value for all data points, which is not distorted by the outliers, and caluclate the mahalanobis distances to the remaining data points based on this mean value. With the help of a statistical distribution, the data points that fall below a certain probability of occurrence can be filtered out. This procedure is repeated until the determinant of the covariance matrix of all remaining data points becomes minimal. This means that the data set does not contain any outliers since the agglomeration of the existing data points does not change any more. Detailed information regarding outlier elimination is given in my previous publication [6].

5.3 Anomaly detection

The initial recorded data defines the initial converter behavior. In the training process of the algorithm, mathematical models are fitted to describe the inital converter behavior. This is done using calculation methods that have already been used for outlier detection. In converter operation, the operating data are compared with the data recorded in the training phase (Fig. 8). All existing relevant environmental and operating conditions are included. It must be ensured that a correct comparison is made between the data recorded in the training process and the newly arriving data set. The anomaly detection is a pre-stage to the root cause detection.

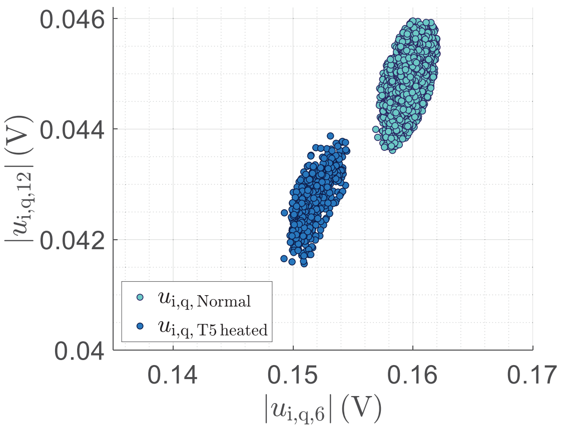

Fig. 8: Anomaly detection

5.4 Root cause detection

In the next step, the cause of the anomaly is detected. This algorithm is trained with simulation data from various fault cases. For data generation, a model is used that simulates aging mechanisms of power converter systems. Therefore, the sensitive parameters described in chapter 3.2 are varied in numerous simulations and the output variables of the current controller are saved. Then, the correlations between the sensitive parameters and the output control variables of the control system are evaluated. Based on these correlations, fitting models are set up that are able to calculate the sensitive parameters in converter operation with the output variables of the controller as an input.

In order to test these created models, intentional changes and manipulations are made to the power semiconductor module. The individual chips of the power semiconductor module are heated through the open viewing window of the circuit board (Fig. 4) using a hot air gun. Figure 10 shows the heating of the positive IGBT T5 of phase c. In Fig. 9, the structure of the power semiconductor module and the chip names can be seen.

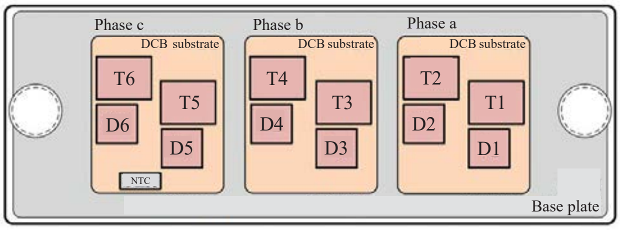

Fig. 9: Power semiconductor module

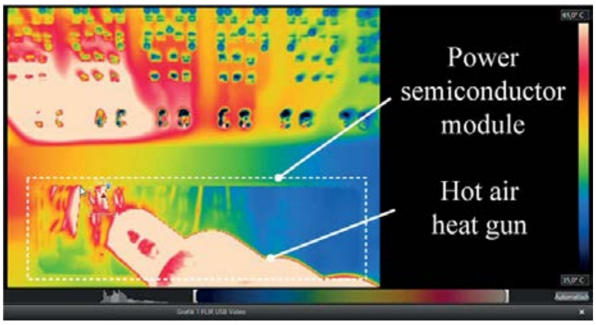

Fig. 10: Heating of individual chips of the power semiconductor module

The temperature range of the power semiconductor chips of the operating point from Tab. 1 is $40\,^\circ\mathrm{C} - 45\,^\circ\mathrm{C}$. The module temperature is approximately $35\,^\circ\mathrm{C}$. Chip T5 is heated a maximum temperature above $80\,^\circ\mathrm{C}$. While the chip is heated, the model results of the root cause detection are determined. The model results of the on state threshold voltage U_f of the collector-emitter path for the heated and unheated chip can be seen in Fig. 11.

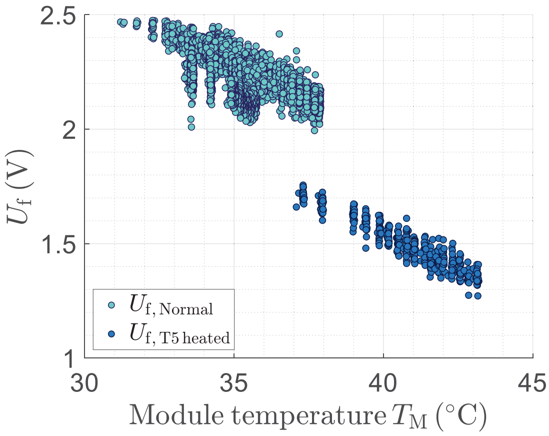

Fig. 11: Model results of the threshold voltage U_f

The module temperature is measured by using the NTC resistor within the module. Alternatively, the chip temperature, which is captured by the thermal imaging camera, can be used for evaluation. It can be seen that the recorded data has a temperature dependence. The on state threshold voltage U_f of the collector-emitter path decreases with increasing temperature. According to [8], the on state collector-emitter voltage is a suitable indicator for detecting certain aging mechanisms such as solder fatigue. However, the limits from which value of the threshold voltage the power converter is still considered functional and from which value the power converter must be replaced has to be determined by extensive field tests. The value calculated by the model does not necessarily have to correspond to the real, physical value. Due to many power converter effects that are not taken into account, such as turn-on and turn-off times, model inaccuracies result. Nevertheless, the value is suitable as an indicator that can be used for certain aging mechanisms.

As an example, only the heating of one power semiconductor chip is shown here. The principle can also be applied to other power semiconductor chips. In order to determine exactly, which chip has heated up, a consideration of the 2^nd harmonic is necessary (Fig. 12). The 2^nd harmonic in the dq frame is an indicator for all types of asymmetry and can be used in order to detect what kind of asymmetry occured. The shift of the data points in the complex plane of the 2^nd harmonic gives an indication of which power semiconductor chip is heated up. Thereby, the positive chips T_1, T_3 and T_5 show a phase shift of around 120° to each other.

6 Conclusion

In this publication, an approach for condition monitoring of power converters, which does not require additional sensors, is presented. Only existing data of a power electronic system are used. The output control variables of the current control system are evaluated. The approach is based on modeling the power converter with inclusion of sensitive parameters. These models are used to perform simulations in which these sensitive parameters are varied. The correlations between the sensitive parameters and the output

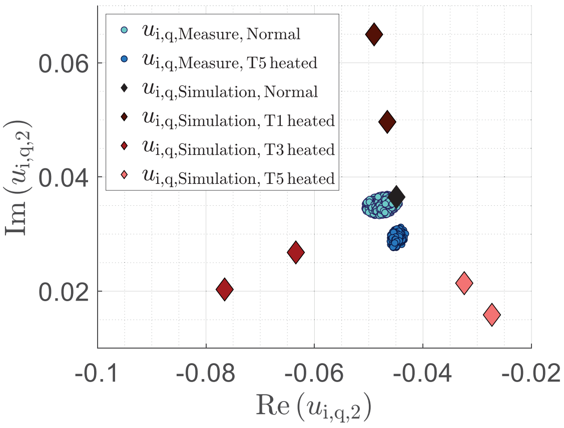

Fig. 12: 2^{nd} harmonic for detection of asymmetry

control variables of the control system are analysed. Based on these correlations, fault detection models are set up that can calculate a change in the sensitive parameter during converter operation. A complete approach to failure detection was presented, including the individual points of data caption, outlier elimination, anomaly detection and root cause detection. In an experiment, individual chips of the power semiconductor module are heated. In order to detect that there was an anomaly in the power semiconductor devices the 6^{th} and the 12^{th} harmonics are investigated. Secondly, by calculating the sensitive parameter, the severity of the fault case can be quantified. Furthermore, by considering the 2^{nd} harmonic, it can be determined in which power semiconductor chip exactly the fault is occurred.

References

[1] U. Choi *and* F. Blaabjerg *and* S. Jørgensen *and* S. Munk-Nielsen *and* B. Rannestad, “Reliability Improvement of Power Converters by Means of Condition Monitoring of IGBT Modules,” *IEEE Transactions on Power Electronics*, 2017.

[2] M. A. Eleffendi *and* C. M. Johnson, “In-Service Diagnostics for Wire-Bond Lift-off and Solder Fatigue of Power Semiconductor Packages,” *IEEE Transactions on Power Electronics*, 2017.

[3] S. Weber *and* M. Schlüter *and* D. Borowski *and* A. Mertens, “Simple Analog Detection of Turn-Off Delay Time for IGBT Junction Temperature Estimation,” *2016 IEEE Energy Conversion Congress and Exposition (ECCE)*, 2016.

[4] M. Denk *and* M. Bakran *and* S. Schafferhans, “Case Sensitive Condition Monitoring of an IGBT Inverter in a Hybrid Car,” *CIPS 2016; 9th International Conference on Integrated Power Electronics Systems*, 2016.

[5] A. Brunko *and* W. Holzke *and* H. Groke *and* B. Orlik *and* N. Kaminski, “Model-Based Condition Monitoring of Power Semiconductor Devices in Wind Turbines,” *2019 21st European Conference on Power Electronics and Applications (EPE ’19 ECCE Europe)*, 2019.

[6] F. Yüce *and* M. Hiller, “Investigation of Bond Wire Lift-Off by Analyzing the Controller Output Voltage Harmonics for the Purpose of Condition Monitoring,” *2020 22nd European Conference on Power Electronics and Applications (EPE’20 ECCE Europe)*, 2020.

[7] M. Hubert *and* M. Debruyne, “Minimum Covariance Determinant,” *Wiley Interdisciplinary Reviews: Computational Statistics*, 2010.

[8] N. Patil *and* D. Das *and* K. Goebel *and* M. Pecht, “Failure Precursors for Insulated Gate Bipolar Transistors (IGBTs),” *IET Seminar Digest*, 2008.

Yüce, F.; Hiller, M.
Condition Monitoring of Power Semiconductors by Means of the Controller Output Voltage Harmonics.
2021. PCIM Europe digital days 2021; International Exhibition and Conference for Power Electronics, Intelligent Motion, Renewable Energy and Energy Management, 3-7 May 2021.
DOI: 10.5445/IR/1000136301

Yüce, F.; Hiller, M.
Condition Monitoring of Power Semiconductors by Means of the Controller Output Voltage Harmonics.
2021. PCIM Europe digital days 2021; International Exhibition and Conference for Power Electronics, Intelligent Motion, Renewable Energy and Energy Management, 3-7 May 2021, 985–992, Institute of Electrical and Electronics Engineers (IEEE).